Artemisia Herba Alba Essential Oil as Green Corrosion Inhibitor for Aluminum in Hydrochloric Acid Solution

Nacer Hechiche, Dalila Boughrara, Abdelaziz Kadri, Nacera Dahmani, Nassima Benbrahim

Anal. Bioanal. Electrochem., Vol. 11, No. 8, 2019, 1129-1147

Analytical & Bioanalytical Electrochemistry

2019 by CEE
www.abechem.com

Full Paper

Artemisia Herba Alba Essential Oil as Green Corrosion Inhibitor for Aluminum in Hydrochloric Acid Solution

Nacer Hechiche,[1,*] Dalila Boughrara,[1] Abdelaziz Kadri,[1] Nacera Dahmani[2] and Nassima Benbrahim[1]

[1]*Laboratoire de Physique et Chimie des Matériaux, Université Mouloud Mammeri de Tizi-Ouzou, Algeria*
[2]*Laboratoire d'Analyse d'Organic Fonctionelle, Faculté de Chimie, Université des Sciences et Technologies Houari Boumediene–Algeria*

*Corresponding Author, Tel.:+213551043445; Fax:+21326221663 or +21326218927
E-Mail: hechiche.n@outlook.fr

Received: 13 June 2019 / Accepted with minor revision: 15 August 2019 / Published online: 31 August 2019

Abstract- *Artemisia herba-alba* essential oil extract was investigated as green inhibitor for aluminum corrosion in 1 M HCl solution. The chemical analysis obtained by gas chromatography and gas chromatography–mass spectrometry, revealed 68 components. The inhibition efficiency was determined by weight loss measurements, potentiodynamic polarization, electrochemical impedance spectroscopy and scanning electron microscope. The results revealed an increase of inhibition efficiency by maximum 92% trough increasing the oil concentration to 3 g/L at 333 K. The oil compounds adsorb by physisorption, follow Langmuir adsorption isotherm and act as mixed type inhibitors. The EIS results confirmed the adsorption mechanism process and the SEM observations.

Keywords– Aluminum, *Artemisia herba-alba*, EIS, SEM, Acid inhibition

1. INTRODUCTION

The aluminum is widely valued for its properties such as light weight, high strength, diversity of its alloys and resistance to corrosion. As a result, aluminum and its alloys play an

important role in industry and scientific technologies. In particular, they are widely used in many applications such as car and truck production, electrical engineering, aerospace and aeronautics [1-3].

The corrosion resistance of aluminum and its alloys is due to the formation of a compact and an adherent alumina layer. However, alumina is amphoteric in nature, when it comes into contact with an aggressive environment (acid pickling bath, chemical etching or industrial cleaning for example) the surface undergoes a severe localized attack which can sometimes lead to significant economic losses and, in addition, accidents [4-7].

A selection of corrosion inhibitors such as organic compounds containing heteroatoms, double and triple bonds and/or aromatic rings, have been and are still being used to prevent this phenomenon [8]. Various classes of organic inhibitors have been reported to have good protection efficiency against materials corrosion in different medium [9-13]. However, even if some synthetic molecules have good anti-corrosive properties, most of them are very toxic to both humans and the environment and are therefore prohibited [14]. To take into account the new environmental protection guidelines, research in the field of corrosion protection of materials is currently focused on biodegradable products commonly known as green inhibitors.

Research in the field of green corrosion inhibitors has been carried out with the aim of developing inhibitors that are acceptable to the environment and less expensive. For this purpose, natural products can be considered as the inexhaustible source. Recently, many plant extracts have been reported in the literature as effective corrosion inhibitors for materials in aggressive environments, in addition to being cheap, renewable source and eco-friendly [15-23].

Artemisia herba-alba is an herbaceous with woody and branched stems, 30 to 50 cm, very leafy with a thick stump. The leaves are small, sessile, pubescent and silvery in appearance. It grows wild in arid areas of the Mediterranean basin. This plant is known as a medicinal and an aromatic plant. In addition, it is an effective inhibitor of foodborne pathogens, as a natural antioxidant, and is used in potential pharmaceutical applications. To the best of our knowledge, there are no studies cited on the inhibitory action of the essential oil (AHAEO) on aluminum corrosion.

In the present study, the composition of *Artemisia herba-alba* oil obtained by hydrodistillation and its inhibitive properties on the corrosion behavior of Al in 1 M hydrochloride acid solution, were investigated by means of weight loss measurement and electrochemical techniques. The influence of temperature was also studied, and some thermodynamic parameters were calculated too.

2. MATERIALS AND METHODS

2.1. Preparation of the plant extract

The flowers and leaves of *Artimisia herba-alba* plant were freshly collected from Guelma in eastern Algeria. Washed several times under running water and rinsed with distilled water before leaving to air dry in the dark for 21 days. After that, a sufficient quantity of distilled water was added to dried plant and brought to a boil for 4 h in order to isolate essential oils by hydrodistillation.

2.2. Materials

The aluminum samples of dimensions (1.5×1.5×0.5 cm) were cut from an aluminum foil with the following chemical composition (in wt. %): 0.15 Fe; 0.06 Si; 0.002 Zn; 0.004 Cu and the balance Al. The aggressive solution (1 mol.L^{-1} HCl) was made from pure-grade HCl provided by Prolabo Chemical Co and deionized water. The inhibitor test solution was prepared by dissolving 30% (V/V) of the as prepared oil in 96% ethanol. The concentrations of inhibitor ranged from 0.5 to 3 g/L, were made by dissolving a desired amount of the inhibitor test solution in HCl (1 mol.L^{-1}) solution.

2.3. Chemical analysis

2.3.1. Gas chromatography

Gas chromatography (GC) analysis was carried out on two capillary columns of different polarities: the apolar HP5 MS ($30\,m \times 0.32\,mm \times 0.25\,\mu m$) and the polar HP WAX ($60\,m \times 0.32\,mm \times 0.15\,\mu m$) using a chromatograph (Hewlett-Packard 6890) equipped with a flame ionization detector (FID). The carrier gas which is helium (He), has a flow rate of 1.2 mL.min^{-1} and 0.9 mL.min^{-1}, respectively, in these columns. The injector and detector temperature is 250 °C. The column temperature is set at 60 °C for 8 min up to 250 °C for 15 min with a programming speed of 2 °C.min^{-1}. The injected volume is 0.2 µL. The percentage of each constituent in the gasoline is calculated by integrating the areas of the chromatogram.

2.3.2. Gas chromatography-mass spectrometry

For gas chromatography-mass spectrometry (GC-MS) analysis, the chromatograph (Hewlett-Packard 6890) equipped with a fused silica HP5 MS column ($30\,m \times 0.32\,mm \times 0.25\,\mu m$) is coupled to an Agilent MSD 5973 mass spectrometer with electronic impact (IE). The temperature and pressure of the source were set at 230 °C and 2×10^{-6} Torr. The ionizing voltage is of 70 eV. The injector and detector temperatures as well as the column temperature programming are identical to those used in GC alone.

2.3.3. Identification of components

The identities of the separated components on the non-polar column were determined by matching their spectral data with those detailed in the Wiley 7N, NIST 02 and NIST 98 libraries.

The results were also confirmed by the comparison of their retention indices RI, relative to C_7-C_{28} n-alkanes assayed under GC-MS in the same conditions as the oil. Some structures were confirmed by available authentic standards analysed under the same conditions described above. The percentage composition of the oils was computed by the normalization method from the GC peak areas. Identification of components was done using volatile oil library coupled with the retention indices of volatile compounds; RI_a, RI_p: retention indices referred to apolar and polar column, determined on HP5 capillary columns; RI_l: retention indices referred to Adams library [25].

2.4. Weight loss method

The aluminum samples were mechanically polished using silicon carbide (Si-C) paper up to 1200 grade under water jet, then ultrasonically degreased in absolute ethanol and finally dried in acetone with cold air. The as polished samples were weighed using a precision analytical balance (10^{-4} g) before immersion for 2 hours in a beaker containing 50 mL of naturally aerated and stagnant solution with different oil concentrations. The temperature is controlled by a thermostat. At the end of each test, the samples are removed from the solution, washed and dried before being weighed again to determine the loss of mass. It should be pointed out that the tests were carried out three times and good reproducibility is being obtained. The corrosion rate (CR) (g/cm^2.s), surface coverage (θ) and the inhibition efficiency ($IE(\%)$) were calculated from equations (1), (2) and (3), respectively:

$$CR = \frac{\Delta m}{S.t} \quad (1)$$

Where Δm is the weight loss, *s* is the specimen surface and *t* the immersion time

$$\theta = \frac{CR - CR'}{CR} \quad (2)$$

Where CR and CR' are the corrosion rates of the aluminum in the absence and presence of inhibitor, respectively.

$$IE(\%) = \theta \times 100 \quad (3)$$

2.5. Electrochemical measurements

The electrochemical tests were carried out in a conventional three-electrode cell, with a platinum counter electrode, Ag/AgCl/(3 mol.L^{-1}), KCl reference electrode and aluminum sample as a working electrode. The sample was covered by an inert resin in order to get an exposed area of 1 cm^2. The electrochemical measurements were performed using a measuring device consisting of an Autolab PGSTAT-30 driven by GPES and FRA 4.9 Software (Eco Chemie, the Netherlands) controlled by a PC.

Two different electrochemical tests were performed to determine the corrosion characteristics. The potentiodynamic polarization testing, in which the potential of the working electrode was swept linearly from negative to positive direction in the range of ±300 mV around E_{corr} value, at a scan rate of 1 mV/s and after 1 hour of immersion time. The inhibition efficiency, $IE(\%)$, was also evaluated by the polarization method using the following equation:

$$IE(\%) = \frac{i'_{corr} - i_{corr}}{i'_{corr}} \times 100 \quad (4)$$

where i'_{corr} and i_{corr} are the corrosion current density without and with AHAEO.

For electrochemical impedance measurements, an ac amplitude voltage of 5 mV at corrosion potential and an applied frequency ranging from 1 kHz to 0.01 Hz has been used. For EIS data modeling and curves fitting method, the Equivalent Circuit Software (Equivcrt) is used. This program is based on non-linear least squares fitting, which allows non-ideal electrochemical behavior to be modeled. The inhibition efficiency, IE, was evaluated using the following equation:

$$IE(\%) = \frac{R_{tc} - R'_{tc}}{R_{tc}} \times 100 \quad (5)$$

Where R_{ct} and R'_{ct} are the charge transfer resistance in inhibitive and uninhibited solutions, respectively.

The double layer capacitance was calculated using equation (6) [24,38]:

$$C_{dl} = Q_{dl} \times (2\pi f_{max})^{n-1} \quad (6)$$

Where, Q_{dl} represents the fitting parameter of the constant phase element (*CPE*), f_{max} is the frequency of the maximum on the imaginary part of impedance vs. frequency and *n* is the CPE exponent (value is in between 0 to 1).

2.6. Morphological observations

The morphological observation of the Al surface was carried out using a scanning electron microscope (JOEL 7500 F) after the surfaces have been mechanically polished and after they have been corroded for 2 h by HCl (1 M) solution with and without AHAEO at 303 K.

3. RESULTS AND DISCUSSION

3.1. Quantification of essential oil constituent

The hydrodistillation result gave an oil yield of 0.95% with a density of 0.87, the resulting oil was stored in a dark glass bottle at 4 °C until analysis.

The analysis of the essential oil of *Artemisia herba-alba* was carried out by GC and GC/MS. Quantification of components was made on the basis of their GC peak areas.

The retention time and percentage of the major volatile compounds are summarized in Table 1. From Morocco to Algeria and Southern Spain, different chemotypes of plants can be found. In this study, the chemical composition of AHAEO is close to the ones cited by Benabdellah et al. [26], for the *Artemisia* from Ain Es-sefra (Algeria, 819 m of altitude) which has the following compounds: β -thujone (31.50–41.23%); camphor: (16.20–24.58%); 1,8-cineol (0.12–9.86%); camphene (3.14–4.25%); chrysanthenone: (0.6–0.9%); α-thujone (2.25–5.55%). For Artimisia located in Ifrane (Morocco), investigated by Boumhara et al. [27], the majors compounds were: 1,8-cineole (35.6%); camphor (24.1%), α-pinene (11.6%), and Camphene (4.9%). Ouachikh et al. [28] reported his study of *Artemisia* from Guenfouda located at the east of Oujda (Morocco) having chrysanthenone (30.6%) and camphor (24.4%) as major components with minor differences compared to this work.

In previous work Dahmani et al. [29] studied the composition of the essential oils of six individual plants of *Artemisia herba alba Asso*, growing wild in six different locations in high table-lands of Algeria: Bordj Bou Arrerridj (BBA, 240 km east of Algiers), Djelfa (DJE, 300 km south of Algiers), M'sila (MSI, 248 km south-eastern of Algiers), Batna (BAT, 425 km east of Algiers), Draa Echih (DRE, 185 km south-eastern of Algiers) and Boussâada (BOU, 360 km south-eastern of Algiers). 132 constituents were identified, predominantly α-thujone (trace–47.1%), camphor (5.6–30.0%), chrysanthenone (trace–13.5%), β-thujone (trace–9.2%), 1,8-cineole (4.1–11.4%), cis-jasmone (0.8–12.1%) and davanone (trace–34.0.%).

In this study, the major constituents of the AHAEO were: Camphor (26.2 %), Chrysanthenone (12.4 %), 1,8-Cineol (8.0 %), α-Thujone (7.8 %) and β-Thujone (6.6 %). The molecular structures of these compounds, dominated by oxygenated monoterpenes, are shown in Figure 1.

Table 1. Chemical composition of major compounds of AHAEO

Compound	RI_a	RI_p	RI_l	Area
1,8-Cineol	1028	1204	1026	8.0
α-Thujone	1105	1409	1101	7.8
β-Thujone	1116	1422	1112	6.6
Chrysanthenone	1127	1505	1124	12.4
Camphor	1148	1514	1141	26.2

RI_a, RI_p : retention indices referred to apolar and polar column, determined on HP5 capillary columns

AHAEO contains several organic compounds of high molecular weight with heteroatom in their chemical structures. The organic compounds have functional groups such as –OR, –C=O, and aromatic ring, which can adsorb on Al surface through nonbonding electron pairs from oxygen atoms as well as π-electrons present in (C=C) double bound, thus reducing the surface area that is available for the attack of the acid solution. However, synergistic effects may play an important role on the inhibition efficiency of AHAEO as an inhibitor. Camphor, the one major component, is known for its good corrosion inhibition efficiency in acid solutions [30].

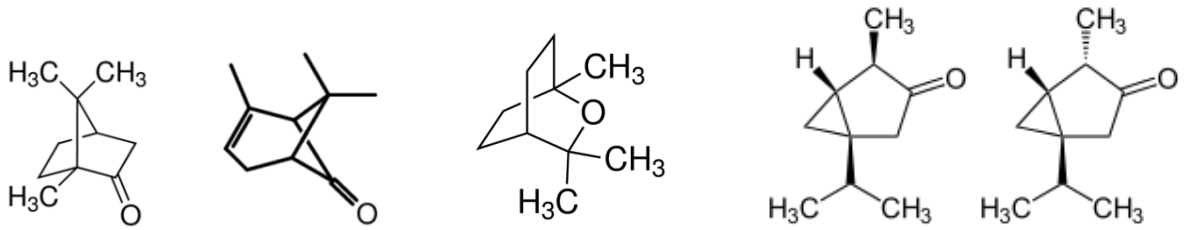

Fig. 1. Molecular structure of the major constituents of the AHAEO

3.2. Weight loss measurements

3.2.1. Effect of inhibitor concentration

The effect of AHAEO concentration on the corrosion of Al in 1 mol.L^{-1} HCl solution was investigated by weight loss measurements at 303 K after 2 h of immersion.

Table 2 exhibits the calculated values of corrosion rates, surface coverage and inhibition efficiency in the absence and presence of different concentrations of *Artemisia* oil according to equations (1), (2) and (3). As can be seen, the corrosion rate of aluminum in 1 mol.L^{-1} HCl solution decreased with the increase of AHAEO concentration. The inhibitory effect of AHAEO is superior at higher concentration; the maximum of 91.60% is attained at 3 g.L^{-1}.

Table 2. Weight loss parameters after 2 h at 303 K

C_{inh} (g.L^{-1})	CR (mg.cm^{-2}.h^{-1})	θ	IE (%)
0	6.43	-	-
0.5	3.26	0.49	49.30
1	2.1	0.67	67.34
2	1.19	0.81	81.49
3	0.54	0.92	91.60

The increase in *IE(%)* with oil concentration is mainly due to the formation of a protective film originated by the strong adsorption of the inhibitor molecules at the metal/solution interface. According to Hmamou et al. [31], the compounds present in the *Artemisia* oil can be adsorbed on the aluminum surface via the electrons pair of an oxygen atom or through the interactions between π- electrons double bounds in aromatic ring and vacant p-orbital of Al.

3.2.2. Adsorption isotherms

To establish the adsorption isotherm that well describe the adsorption of AHAEO, the degree of surface coverage (θ) obtained from the weight loss data using eq. (2), were fitted into the most well-known adsorption isotherms including the Temkin, Langmuir, Frumkin and Freundlich models [24,32]:

Temkin isotherm $$exp(-2a\theta) = K_{ads}\, C \quad (7)$$
a is constant of interaction between adsorbed particules.

Langmuir isotherm $$\frac{C}{\theta} = \frac{1}{K_{ads}} + C \quad (8)$$

Frumkin isotherm $$\frac{\theta}{(1-\theta)} exp(2a\theta) = K_{ads}\, C \quad (9)$$

Freundlich isotherm $$ln\ \theta = lnK_{ads} + \alpha lnC \quad (10)$$
α *is the degree of nonlinearity* $0 < \alpha < 1$

Where K_{ads} ($L.g^{-1}$) is the equilibrium constant for adsorption process.

The best correlation between the isotherm functions and experimental results was achieved using the Langmuir adsorption isotherm given by equation (8). As can be seen from Figure 2, the plot of C/θ versus C is linear (both slope value and linear correlation coefficient (R) are close to 1). The model of adsorption mechanism explains the inhibitive action of AHAEO on the aluminum corrosion in HCl (1 $mol.L^{-1}$) medium which acts by the formation of a monolayer barrier of active compounds present in the oil at the aluminum surface.

The K_{ads} value of AHAEO at 303 K, deduced from the Langmuir isotherm plot is 1.69 $L.g^{-1}$. On the other hand, this constant value was directly used to calculate the standard free energy of adsorption (ΔG^0_{ads}) of the inhibitor molecules, using the following equation :

$$K_{ads} = \frac{1}{C_{H_2O}} \exp\left(\frac{-\Delta G^0_{ads}}{RT}\right) \quad (11)$$

where C_{H_2O} represents the concentration of water in solution. It should be noted that the unit of C_{H_2O} have to be identical to that of K_{ads} which in consequence implies that the unit of C_{H_2O} is $g.L^{-1}$ (with value of approximate 1.0×10^3) [33]. R is the universal molar gas constant (8, 31 $J.mol^{-1}.K^{-1}$) and T the temperature is in K.

For ΔG°_{ads} values up to -20 kJ.mol^{-1}, the mechanism of adsorption is compatible with physisorption, in which case inhibition results from electrostatic interactions between the charged metal surface and the charged molecules of the inhibitor, while for those of about -40 kJ mol^{-1} or higher are correlated with chimisorption [34,35].

In this work, for a temperature of 303 K, the obtained values of ΔG°_{ads} is -18,71 kJ.mol^{-1}. The negative sign of ΔG°_{ads} ensures the spontaneity of the adsorption process and the value indicates that the inhibitor's molecules are physically adsorbed.

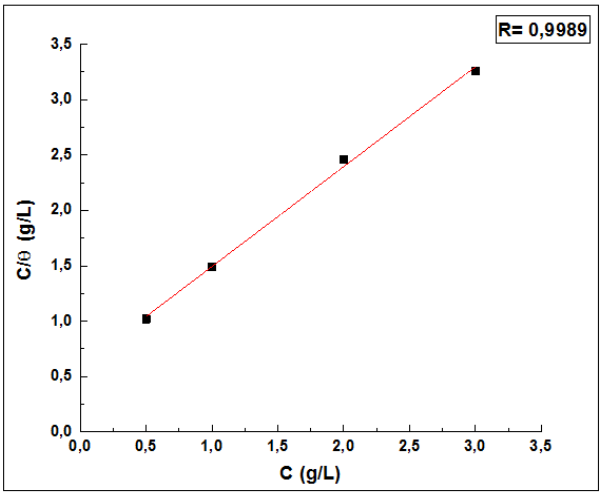

Fig. 2. Langmuir adsorption isotherm plot for AHAEO on Al for 2 h in 1 M HCl at 303 K

3.2.3. Effect of temperature

In order to estimate the stability of the adsorbed inhibitor's molecules, the influence of temperature on the Al corrosion was studied in the absence and presence of the optimum concentration (3 g.L^{-1}) of AHAEO between 303 and 333 K during 2 h, using weight loss measurements (Table 3).

Table 3. Corrosion rate between 303 and 333 K in absence and presence of 3 g.L^{-1} of oil after 2 h of immersion

T ***(K)***	***CR*** ***(mg.cm^{-2}.h^{-1})***	***CR′*** ***(mg.cm^{-2}.h^{-1})***	***IE*** ***(%)***
303	6,43	0,54	91,6
313	9,04	2,01	77,75
323	19,88	5,82	70,72
333	22,49	9,44	58,03

As can be clearly seen, the temperature affects the inhibition efficiency. The increasing temperature leads to a decrease in inhibition efficiency, which may be attributed to either the enhanced desorption of inhibitor molecules with increasing temperature from Al surface or to the degradation and decomposition of its organic content.

The Al corrosion rate decreases in the acidic medium in presence of the inhibitor at 3 $g.L^{-1}$ compared to the blank. CR value is more pronounced with the increase of temperature both in the presence and absence of inhibitor. The temperature dependence of the corrosion rate, was estimated by the apparent activation energy, E_a^0, calculated using the Arrhenius equation [36]:

$$logCR = \frac{-E_a^0}{2.303\ RT} + log\lambda \quad (12)$$

where λ is the frequency factor.

From the Arrhenius plots, shown in Figure 3, the fitted E_a value obtained for uninhibited and inhibited acid solution, increases from 37,53 $KJ.mol^{-1}$ to 80,04 $KJ.mol^{-1}$, respectively. Authors in literature [37,38] have interpreted this increasing to the presence of higher barrier energy for the reaction of aluminum corrosion by the formation of a physical adsorbed film of inhibitor, slowing down the Al dissolution.

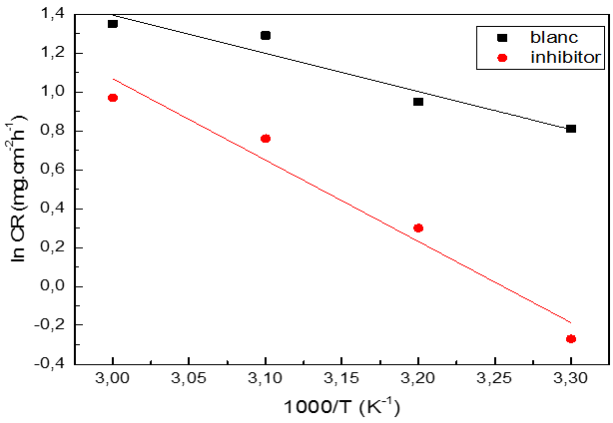

Fig. 3. Arrhenius plots for blank and 3 $g.L^{-1}$ of AHAEO

3.3. Morphological analysis

In order to support our findings, the SEM micrographs for Al surfaces were shown in Figure 4 for Al in 1 M HCl in the absence and presence of AHAEO.

Before immersion in the test solutions (Figure 4a), the metal surface appears uniform with some of polishing lines. However, after 1 h of Al immersion in HCl without inhibitor, the SEM image shown in Figure 4b, reveals a strongly damaged surface. The Al surface is highly corroded by the rigorous attack of HCl (pH ≈ 0). Furthermore, the surface appears rather rough.

However, the presence of 1 and 3 g.L^{-1} of AHAEO, reduce increasingly the damage on the Al surface as shown by SEM images of Figure 4c and 4d, respectively. The presence of the inhibitor revealed some pits whose number decreases with AHAEO concentration. The optimum concentration (Figure 5d) exhibits a smooth surface indicating restricted corrosion. These improvements in surface confirm the formation of an adsorbed film of AHAEO on the Al surface which protects and isolates it from the corrosive solution. It is evident from the surface morphology, that the addition of the inhibitor protects the Al surface. These results are in good agreement with the weight loss measurements.

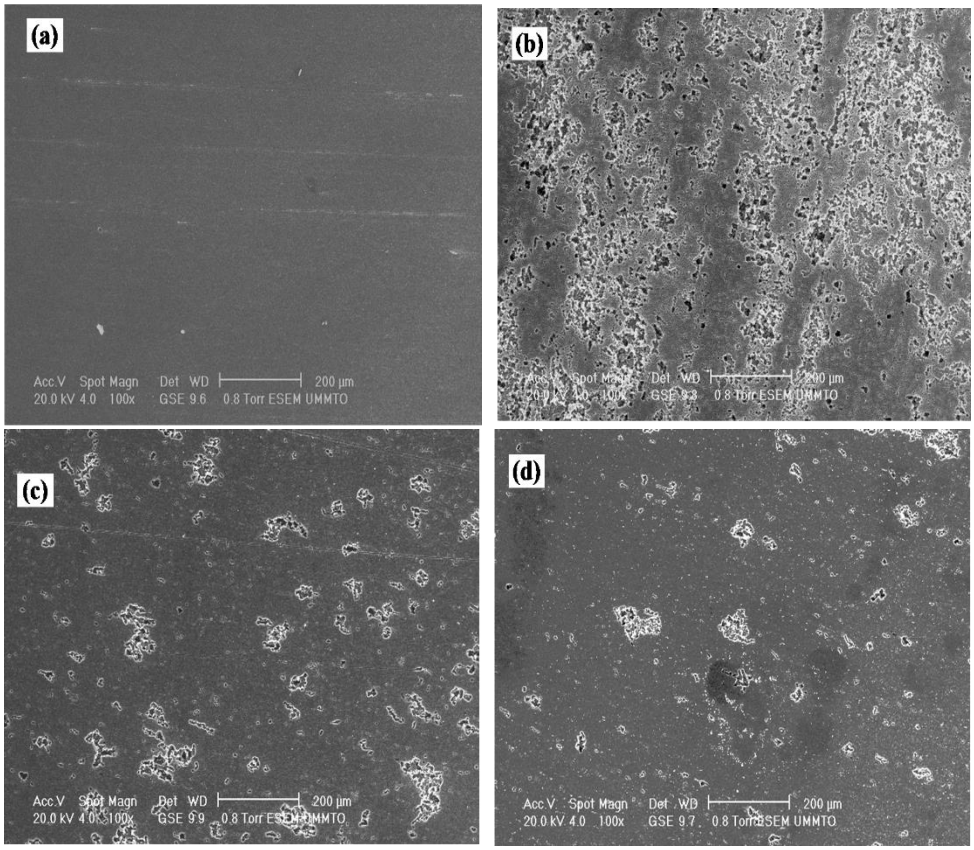

Fig. 4. SEM micrographs of Al surface at 303 K; (a) Polished surface, after 2 h in (b) 1 M HCl and (c) 1 M HCl +3 g.L^{-1} of AHAEO

3.4. Polarization measurements

Figure 5 shows the potentiodynamic polarization curves recorded with an Al electrode immersed in HCl solution (1 mol.L^{-1}) at 303 K, in the absence and presence of different AHAEO contents.

It can be clearly seen that with the increase of AHAEO inhibitor concentration, the polarization curves were shift into more negative values of potential and the cathodic and

anodic current densities toward lower values in comparison to the blank, with predominant decrease at cathodic site. This may suggests a mixed type of corrosion inhibitor.
In concentrated acidic medium, only H^+ ions are taken in consideration in the cathodic process:
$2H^+ + e^- \rightarrow H_2$

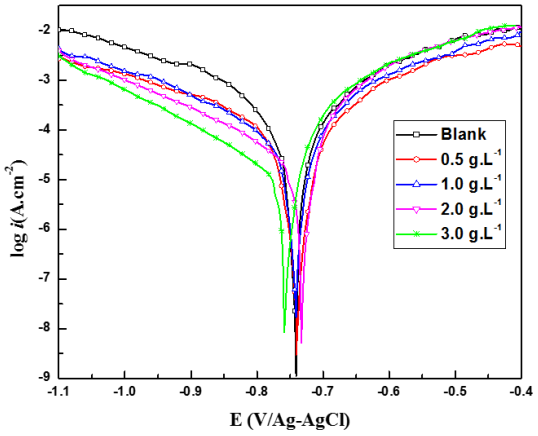

Fig. 5. Potentidynamic polarization curves for Al after 1 h of immersion in 1 M HCl with and without AHAEO at 303 K

On the anodic polarization curves, no passive region was observed, due to the dissolution of the oxide film of alumina in the hydrochloride acid media (pH around 0). This is a shape for uniformly corroding metal: $Al \rightarrow Al^{3+} + 3e^-$ followed by the formation of $AlCl_3$. It could be concluded that the adsorption-desorption of AHAEO, in competition with the anodic dissolution of Al, affect slightly the rate of the anodic dissolution of Al. The polarization parameters, the corrosion potential (E_{corr}), the cathodic and anodic Tafel slopes (b_c and b_a), after E_{corr} by ±50 mV, the corrosion current densities (i_{corr}), obtained by extrapolating the Tafel lines to E_{corr}, are reported in Table 4.

Table 4. Potentiodynamic polarization parameters for Al in HCl (1 mol.L^{-1}) in the absence and presence of different concentrations of AHAEO at 303 K

C_{inh} (g.L^{-1})	E_{corr} (mV/AgAgCl)	$-b_c$ (mV/dec)	b_a (mV/dec)	i_{corr} (µA.cm^{-2})	θ	IE (%)
0	-740	121	100	112	-	-
0.5	-743	139	91	44	0,61	61
1	-745	145	78	41	0,63	63
2	-735	150	56	21	0,81	81
3	-758	132	55	10	0,92	**92**

We can notice a slight shift of the corrosion potential, E_{corr}, in the cathodic direction with the rise of AHAEO concentration. It was reported that, when the shift in E_{corr} is more than ±85 mV compared to the value of the blank solution, the inhibitor can be considered as a cathodic or anodic type, if the displacement in E_{corr} is lower than ± 85 mV, the corrosion inhibitor may be regarded as a mixed type [39]. In our study, the maximum displacement in E_{corr} value was 18 mV, relative to the blank solution, which indicates that these compounds act as mixed-type inhibitors with predominant cathodic effectiveness.

Moreover, the cathodic Tafel curves appear as parallel lines with b_c values rising from -120 to 150 mV with increasing AHAEO concentration and small changes were noticed compared to blank (-120 mV). The fact b_c values are equal in uninhibited and inhibited solution suggests that the inhibitor does not modify the hydrogen evolution mechanism, which occurs generally through a charge transfer mechanism with a theoretical value of b_c equal to -120 mV..

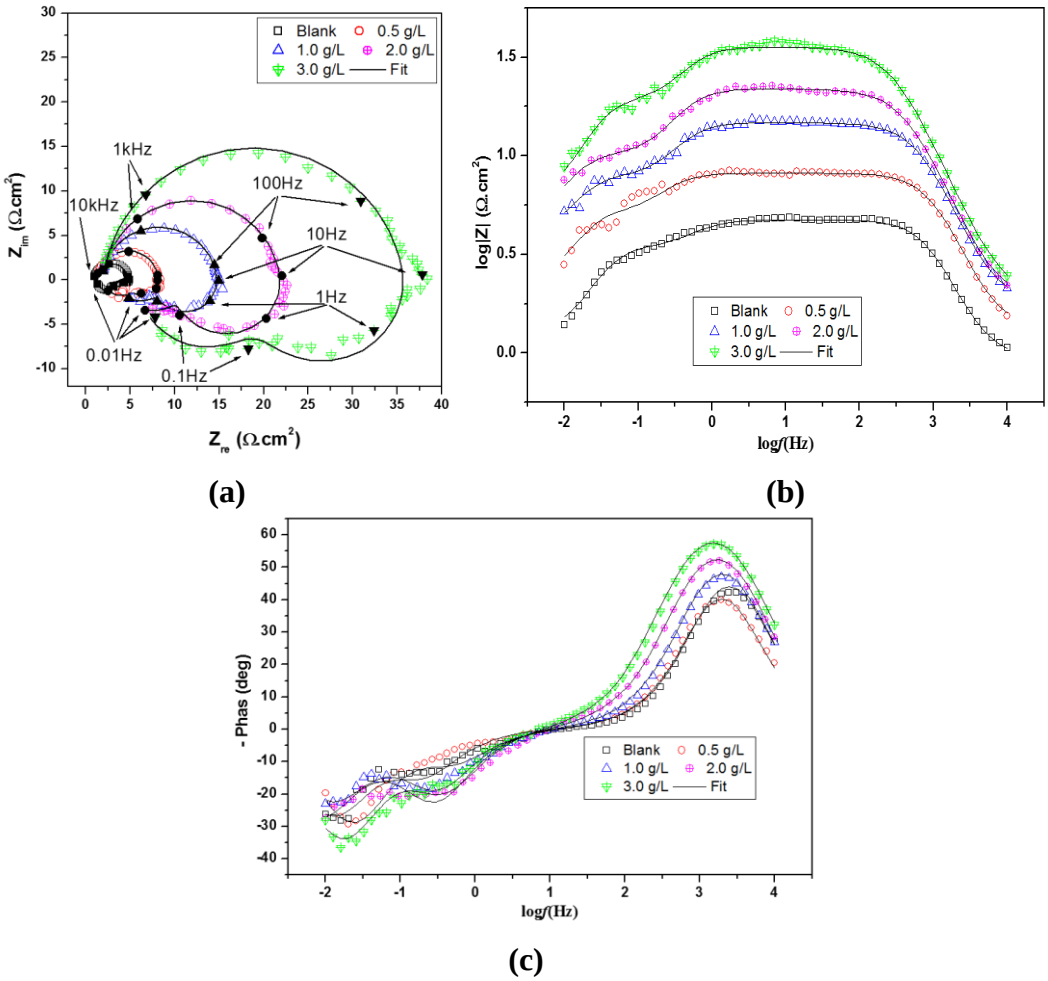

Fig. 6. EIS diagrams for aluminum in 1 M HCl solution in absence and presence of AHAEO, obtained after 1 h of immersion at open circuit potential and at 303 K. a) Nyquist; b) Bode modulus and c) Bode phase representations

So, the inhibitors act just by blocking the electrode surface. For anodic dissolution, the decrease in anodic Tafel slopes b_a , with increasing of inhibitor concentration, suggests that the inhibitor affected the kinetics of the anodic process. is probably due to the desorption of AHAEO.

Finally, it should be mentioned that the decrease in the corrosion current density, i_{corr}, with the increase of inhibitor concentration, give rise to inhibitive efficiency of AHAEO on aluminum in HCl (1 mol.L^{-1}) solution that reaching maximum value of 92.7% at 3 g.L^{-1}.

The results are in good agreement with the decrease in corrosion rate (CR) obtained from weight loss measurements.

3.5. Electrochemical impedance spectroscopy

Figure 6 shows the impedance diagrams, in the Nyquist (Figure 6a) and Bode representations (Figure 6b,c) for Al electrode in contact with a 1 M HCl in the absence and presence of different concentrations of AHAEO. The diagrams were recorded after 1 hour of immersion at open circuit potential and at 303 K.

As can be seen from the figure, in the frequency range of measurements, all impedance spectra have nearly the same characteristics, demonstrating that almost no change in the corrosion mechanism happened when concentration was changed. We can discriminate nearly three frequency time constants, the impedance spectra in Nyquist presentation present a large capacitive loop at higher frequencies (HF) followed by two inductive loops at lower frequencies (LF). In Bode presentation, observation of a large and flattened magnitude of the impedance and multiple maxima in phase angle diagram, indicate that the data must be interpreted in terms of more than one process, more than one time constant is required to fully describe the system.

It is also interesting to note that the impedance of the system depends on the AHAEO concentration; remarkable increase in impedance magnitude with AHAEO concentration is noticed. At HF, the capacitive loop may be related to both charge transfer of the corrosion process and double layer behavior. Whereas, inductive loop at LF is always reported for Al in HCl solution inhibited by organic compounds [32,40-43].

Since the same features were observed for all the electrodes (with and without inhibitor), the inductive loops shown in the present work, may be associated to the electrical activity of the electrode surface during the corrosion process (absorption of chloride ions, dissolution, pits propagation and localized hydrogen evolution). Lower diameters of capacitive and inductive loops are observed in blank solution (without AHAEO), which suggest higher charge transfer and higher deterioration of the protective film of corrosion products. Otherwise, severe pitting corrosion occurred as already confirmed by SEM analysis (Figure 4). Through adding inhibitor, the size of the capacitive and inductive loops altered. The increase of AHAEO concentration leads to increase of diameters of both capacitive and inductive loops, which indicate that with

the rise of the inhibitor concentration, charge transfer process and pit propagation mechanism are impeded. So, based on SEM analysis, a perfect correlation may be found between the inductive loop magnitude and the propagation of the pitting corrosion.

To acquire interfacial parameter values, a nonlinear least squares fitting of impedance spectra was employed. The equivalent circuit was established on the basis of a general knowledge of the physical events which can occur at the interface. The best agreement between experiment and fitting were obtained with an equivalent circuit illustrated in Figure 7.

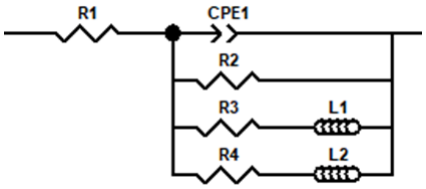

Fig. 7. The equivalent circuit used to fit the obtained impedance spectra

Solid lines in Figure 6, show the results from fitting the experimental data according to the presented model. In this model, (R_s) represents the solution resistance, (R_{ct}) the charge transfer resistance, (CPE_{dl}) the pseudo double layer capacitance, (R_{ind1} , L_1) and (R_{ind2} , L_2) are the two branches characterizing the inductive loops. R_{ind1} and L_1 are the inductive resistance and the inductance, respectively. The second parallel branch of the circuit is included to achieve an optimal fit between the measured impedance and simulation model. Constant phase element (*CPE*) was introduced instead of pure capacitance to take into account the non-ideal behaviour of the capacitive element. Appearance of the CPE is a consequence of the dispersion of time constants which can originate from different physical phenomena, such as the inhomogeneity of the Al surface [44]. The equivalent circuit parameters values obtained by fitting are regrouped in Table 5.

As can be clearly seen, R_{ct} values increase significantly with the increase of AHAEO concentration. This change may be correlated to the gradual increase of inhibitor molecules and therefore to a decrease in the number of active sites required for the corrosion process.

Values of C_{dl} in inhibitive solution are low (around 20 µF.cm^{-2}) below the known value of a double layer capacitance (~50 µF.cm^{-2}), so the HF loop may be the result from both charge transfer and a film effect of AHAEO. C_{dl} decreases with AHAEO concentration signifying that higher presence of AHAEO greatly contributes in the blockage of the charge transfer process and prevents the destruction of the Al surface. The exponent of the CPE (n) increased with AHAEO concentration from 0.817 to 0.883. It attained the maximum value at higher concentration (3 g.L^{-1}), suggesting the decrease of the surface heterogeneity due to the coverage of the most active sites by the adsorbed molecules of the inhibitor. The parameters R_{ind} and L_{ind} associated with the inductive loops increase with increase in AHAEO concentration indicating that AHAEO inhibits the absorption of Cl^- and prevents the corrosion process.

As stated before, Camphor is a major component of AHAEO, this molecule plays an important role in the inhibition corrosion mechanism. Very recently, Bourazmi et al. [30] have shown by theoretical calculations that the geometry of this molecule is directly involved in the corrosion inhibition activity of the electrode. In fact, camphor in its ground state, the nature of its molecular orbitals, HOMO (Highest Occupied Molecular Orbital) and LUMO (Lowest Unoccupied Molecular Orbital), is responsible of the decrease in the number of active sites necessary for the corrosion reaction. Consequently, the inhibition efficiency rises with the inhibitor concentration and reaches a maximal value of 89 % at 3 $g.L^{-1}$.

The EIS results are in good agreement with weight loss measurements and potentiondynamic polarization as shown in Figure 8.

Table 5. Electrical parameters and inhibition efficiencies for Al in 1 M HCl solution in absence and presence of various concentrations of AHAEO at 303 K

C_{inh} ($g.L^{-1}$)	R_s ($\Omega.cm^2$)	R_{ct} ($\Omega.cm^2$)	C_{dl} ($\mu F.cm^{-2}$)	*n*	R_{ind1} ($\Omega.cm^2$)	L_1 ($H.cm^2$)	R_{ind2} ($\Omega.cm^2$)	L_2 ($H.cm^2$)	*IE* (%)
0	0.96	4,1	48.46	0,817	3.5	3,12	1.3	12.4	-
0,5	1.32	8,3	23.84	0,818	5.25	10.94	2.5	41.1	50.60
1	1.78	14,6	18.84	0.824	7.6	9.87	4.9	81.8	71.91
2	1.8	21,8	17.86	0.880	11	13.85	6.3	136.2	81.19
3	1.86	36	15.56	0.883	19.5	23.12	*7.5*	122.3	88.61

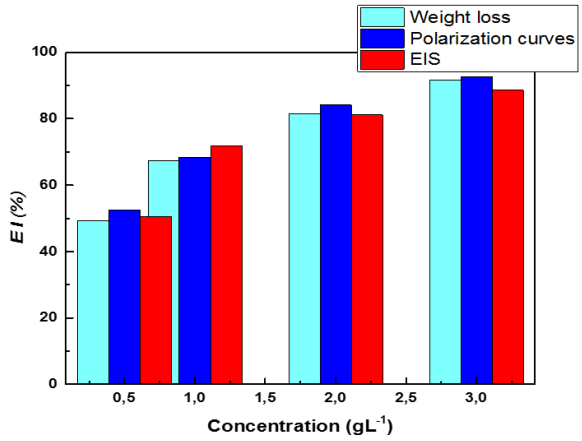

Fig. 8. Bar plots of the inhibition efficiencies vs. inhibitor concentration obtained from weight loss measurements, polarization curves and electrochemical impedance spectroscopy

4. CONCLUSION

GC-MS analysis provides the major constituents of *Artemisia herba-alba* oil which are Camphor (26.2%), Chrisanthenone (12.4%), (1,8-Cineol) 8.00%, (α-Thujone) 7.8% and (β-15

Thujone) 6.6%. The weight loss measurements indicated that inhibition efficiency (IE %) increase with AHAEO concentration and decrease with temperature. Maximum value of inhibition efficiency (92.7%) was reached at 3 $g.L^{-1}$. The studies of the adsorption process showed a Langmuir adsorption process with a physisorption aspect, established by the value of the adsorption energy ($\Delta G°_{ads}$ = -18.71 $kJ.mol^{-1}$ at 30 °C). Th_e increase of the activation energy ($Ea0$) of the Al dissolution in presence of AHAEO confirms the physisorption aspect of the adsorption. SEM studies revealed improvements in Al surface in presence of AHAEO which confirm the formation of an adsorbed and protective barrier of AHAEO molecules. The polarization studies showed that AHAEO acts as mixed-type inhibitor without changing the hydrogen evolution mechanism. From EIS measurement it is clear that the charge transfer resistance increase with the inhibitor concentration and charge transfer process and pit propagation mechanism are impeded. SEM analysis allows a perfect correlation between the magnitude of the inductive loop and the propagation of pitting corrosion. Good agreement was obtained between the different methods employed in this study and showed that *Artemisia herba-alba* can be a good candidate for aluminum corrosion protection in hydrochloric acid medium.

Acknowledgement

The authors wish to acknowledge Boudinar Salem, researcher from Laboratory of Physics and Chemistry of Materials, Faculty of Physics at Mouloud Maameri University of Tizi-ouzou-Algeria, for providing SEM observations.

REFERENCES

[1] M. Abdallah, E. M. Kamar, S. Eid, and A.Y. El-Etre, J. Mol. Liq. 220 (2016) 755.
[2] T. Dursun, and C. Soutis, Materi. Design 56 (2014) 862.
[3] J. Hirsch, and T. Nonferr. Metal. Soc. 24 (2014) 1995.
[4] O. K. Abiola, and Y. Tobun, Chin. Chem. Lett. 21 (2010) 1449.
[5] M. H. Hussin, and M. J. Kassim, Mater. Chem. Phys. 125 (2011) 461.
[6] J. Halambek, A. Žutinić, and K. Berković, Int. J. Electrochem. Sci. 8 (2013) 11201.
[7] S. Şafak, B. Duran, A. Yurt, and G. Türkoğlu, Corros. Sci. 54 (2012) 251.
[8] D. Prabhu, and P. Rao, J. Environ. Chem. Eng. 1 (2013) 676.
[9] F. S. DE Souza, and A. Spinelli, Corros. Sci. 51 (2009) 642.
[10] X. Li, X. Xie, S. Deng, and G. Du, Corros. Sci. 87 (2014) 27.
[11] M. Gopiraman, N. Selvakumaran, D. Kesavan, and R. Karvembu, Prog. Org. Coat. 73 (2012) 104.
[12] D. Daoud, T. Douadi, H. Hamani, S. Chafaa, and M. Al-Noaimi, Corros. Sci. 94 (2015) 21.

[13] H. Gerengi, M. M. Solomon, M. Kurtay, G. Bereket, K. Goksen, M. Yıldız, and E. Kaya, J. Adhes. Sci. Technol. 32 (2018) 207.
[14] A. A. Rahim, E. Rocca, J. Steinmetz, and M. J. Kassim, Corros. Sci. 50 (2008) 1546.
[15] A. Khadraoui, A. Khelifa, K. Hachama, and R. Mehdaoui, J. Mol. Liq. 214 (2016) 293.
[16] J. Halambek, K. Berković, and J. Vorkapić-Furač, Mater. Chem. Phys. 137 (2013) 788.
[17] D. I. Njoku, I. Ukaga, O. B. Ikenna, E. E. Oguzie, K. L. Oguzie, and N. Ibisi, J. Mol. Liq. 219 (2016) 417.
[18] S. A. Umoren, I. B. Obot, E. E. Ebenso, and N. O. Obi-Egbedi, Desalination. 247 (2009) 561.
[19] M. Nasibi, M. Mohammady, A. Ashrafi, A. A. D. Khalaji, M. Moshrefifar, and E. Rafiee, J. Adhes. Sci. Technol. 28 (2014) 2001.
[20] A. M. Abdel-Gaber, E. Khamis, H. Abo-ElDahab, and S. Adeel, Mater. Chem. Phys. 109 (2008) 297.
[21] E. I. Ating, S. A. Umoren, I. I. Udousoro, E. E. Ebenso, and A. P. Udoh, Green. Chem. Lett. Rev. 3 (2010) 61.
[22] A. Khadraoui, A. Khelifa, L. Touafri, H. Hamitouche, and R. Mehdaoui, J. Mater. Environ. Sci. 4 (2013) 663.
[23] H. Hachelef, A. Benmoussat, A. Khelifa, D. Athmani, and D. Bouchareb, J. Mater. Environ. Sci. 7 (2016) 1751.
[24] X. Li, S. Deng, and H. Fu, Corros. Sci. 53 (2011) 1529.
[25] R. P. Adams, Identification of Essential Oil Components by Gas Chromatography/Mass Spectroscopy, (2007) No.Ed.4 pp.viii + 804 pp.
[26] M. Benabdellah, M. Benkaddour, B. Hammouti, M. Bendahhou, and A. Aouniti, Appl. Surf. Sci. 252 (2006) 6212.
[27] K. Boumhara, H. Harhar, M. Tabyaoui, A. Bellaouchou, A. Guenbour, and A. Zarrouk, J. Bio. Tribo-Corrosion 5 (2019) 8.
[28] O. Ouachikh, A. Bouyanzer, M. Bouklah, J. M. Desjobert, J. Costa, B. Hammouti, and L. Majidi, Surf. Rev. Lett. 16 (2009) 49.
[29] N. Dahmani-Hamzaoui, and A. Baaliouamer, J. Essent. Oil. Res. 27 (2015) 437.
[30] H. Bourazmi, M. Tabyaoui, L. Hattabi, Y. El Aoufir, E. Ebenso, and A. Ansari, J. Mater. Environ. Sci. 9 (2018) 1058.
[31] D. B. Hmamou, R. Salghi, A. Zarrouk, H. Zarrok, R. Touzani, B. Hammouti, and A. El Assyry, J. Environ. Chem. Eng. 3 (2015) 2031.
[32] A. Khadiri, A. Ousslim, K. Bekkouche, A. Aouniti, A. Elidrissi, and B. Hammouti, Electrochim. Acta 32 (2014) 35.
[33] S. Deng, and X. Li, Corros. Sci. 64 (2012) 253.
[34] I. M. Mejeha, A. A. Uroh, K. B. Okeoma, and G. A. Alozie, African J. Pure Appl. Chem. 4 (2010) 158.

[35] A. I. Obike, K. J. Uwakwe, M. C Ebeagwu, P. C. Okafor, and E. C. Ogili, J. Phys. Chem. Biophys. 8 (2018) 264
[36] S. A. Umoren, I. B. Obot, and N. O. Obi-egbedi, J. mater. Sci. 44 (2009) 274.
[37] N. K. Gupta, M. A. Quraishi, P. Singh, V. Srivastava, K. Srivastava, C. Verma, and A. K. Mukherjee, Anal. Bioanal. Electrochem. 9 (2017) 245.
[38] L. A. Nnanna, B. N. Onwuagba, I. M. Mejeha, and K. B. Okeoma, Afr. J. Pure Appl. Chem. 4 (2010) 011.
[39] G. Lyberatos, and L. Kobotiatis, Corrosion 47 (1991) 820.
[40] E. A. Noor, Mater. Chem. Phys. 114 (2009) 533.
[41] D. G. Ladha, P. M. Wadhwani, M. Y. Lone, P. C. Jha, and N. K. Shah, Anal. Bioanal. Electrochem. 7 (2015) 59.
[42] C. M. Brett, Corros. Sci. 33 (1992) 203.
[43] S. S. A El Rehim, H. H. Hassan, and M. A. Amin, Mater. Chem. Phys. 70 (2001) 64.
[44] M. Lebrini, M. Lagrenée, H. Vezin, M. Traisnel, and F. Bentiss, Corros. Sci. 49 (2007) 2254.